Строительные материалы и изделия
Construction Materials and Products

journal homepage: https://bstu-journals.ru

ISSN
2618-7183

DOI: 10.58224/2618-7183-2026-9-4-7

Organomineral thermal insulation composite with reduced flammability based on sodium silicate and a polyurethane foam matrix

Lipka P.A. * [1], Bruyako M.G. [1], Kozlova I.V. [1], Samchenko S.V. [1], Korshunov A.V. [1], Taran G.S. [2]

[1] National Research Moscow State University of Civil Engineering, Russia,
[2] Kurnakov institute of General and Inorganic Chemistry, Russian Academy of Sciences, Russia

Abstract. This article is devoted to the study of an organomineral thermal insulation composite based on a rigid polyurethane foam (PUF) matrix and a flammability-reducing silicate component-sodium metasilicate pentahydrate ($Na_2SiO_3 \cdot 5H_2O$, 0.9-1.25 mm fraction). The physicochemical regularities of the interaction between the silicate component and isocyanate, the fire-retardant mechanism of the silicate component, and its effect on the thermal properties and flammability of the composite have been investigated.

A chemical interaction between the isocyanate functional groups of the reactive mixture and the water contained in the silicate component was established to occur at the phase boundary.

The fire-retardant mechanism of the silicate component consists in the endothermic release of crystallization water (70-170 °C), which induces intumescence of the metasilicate, resulting in the formation of a porous heat-insulating barrier.

The silicate component does not alter the fundamental decomposition mechanism of the polyurethane, yet it shifts the stages of thermo-oxidative degradation to lower temperatures (by 15-85 °C). The final residue increases up to 8.1 times (from 3.6 to 29.1 wt%), which directly corresponds to the contribution of the dehydrated silicate.

Flammability tests demonstrated that when the silicate component content exceeds 45%, the material achieves a UL-94 V-0 rating, and the limiting oxygen index (LOI) increases from 17.8 to 26.6 at a 90% silicate component loading.

The obtained results substantiate the effectiveness of using sodium silicate crystalline hydrate as a fire-retardant additive, and it can be recommended for the development of composites based on other polymer matrices.

Keywords: silicate component, sodium metasilicate, crystalline hydrate, dispersion, pore structure, foaming, rigid polyurethane foam, combustibility

*Corresponding author E-mail: petr.lipka2020@gmail.com

Received April 21, 2026; Received in revised form June 23, 2026; Accepted July 25, 2026

Please cite this article as: Lipka P.A., Bruyako M.G., Kozlova I.V., Samchenko S.V., Korshunov A.V., Taran G.S. Organomineral thermal insulation composite with reduced flammability based on sodium silicate and a polyurethane foam matrix. Construction Materials and Products. 2026. 9 (4). 7. DOI: 10.58224/2618-7183-2026-9-4-7

1. INTRODUCTION

Reducing energy consumption during the operation of buildings and structures is one of the priority areas. Thus, mandatory assignment of an energy efficiency class for all newly commissioned multi-apartment residential buildings has been in effect since 2016. An effective way to reduce energy costs is the use of thermal insulation materials, the most efficient of which are polymeric ones. However, a drawback of the latter is their flammability, which limits the range of their application. Accordingly, work is underway to develop new materials and to modify existing ones. Of particular interest are studies aimed at creating organomineral thermal insulation composites. Methods are known for introducing liquid-glass compositions (potassium, lithium, and sodium) into the reactive system for producing polyurethane foams, where liquid glass is introduced into the mixture to participate directly in the chemical reaction with polyisocyanate. This can result in the formation of interpenetrating polymer networks and new organomineral compounds that enhance the thermal stability of polyurethane foam [1-3]. However, the high water content in the solutions, which acts as a chemical blowing agent in the system, does not allow liquid glasses to be introduced in significant amounts. For this reason, we have previously proposed the use of crystalline hydrate forms of sodium silicates and investigated the effect of introducing sodium metasilicate pentahydrate ($Na_2SiO_3 \cdot 5H_2O$) into the reactive component system for producing PUF on the processing and physical-mechanical characteristics of the resulting composites [4, 5].

It was found that the addition of the silicate component leads to an increase in the foaming ratio; that is, the isocyanate (as a reactive component) presumably interacts with the chemically bound water of the pentahydrate at the phase boundary, with the release of carbon dioxide (CO_2). In this case, the pores surrounding the additive and being in contact with it exhibit an ellipsoidal shape, with their long axis oriented perpendicular to the additive surface. Although gas "bubbles" normally tend to minimize the gas-polymer interfacial area due to surface tension forces, forming a spherical shape, expanding stepwise, approaching each other, and forming polyhedra, in this case the interaction with the crystalline hydrate water of the additive is likely to occur, which creates a stretching vector of the polymer framework perpendicular to the additive surface. At the same time, the resulting pores uniformly surround the additive and form a stable "adhesion node".

The purpose of the study: establishing the physicochemical regularities of the interaction between the silicate component and isocyanate, determining the fire-retardant mechanism of the silicate component, and assessing its effect on the thermal properties and flammability of the composite.

2. METHODS AND MATERIALS

Materials

The following raw materials were selected for the study:

Isocyanate component (IC): polyisocyanate «Wannate PM-200» (Wanhua, China), which is a mixture of diphenylmethane-4.4'-diisocyanate (MDI) with its isomers and homologues. Its molecular weight ranges from 350 to 400 amu, NCO group content from 30.5 to 32%, density 1240 kg/m^3 (CAS number: 9016-87-9).

Polyol component (PC): polyether «Izolan A-359» (TU 20.16.40-920-97445105-18), density 1100 kg/m^3, cream time 35-65 s, gel time 150-300 s, free rise density 33-50 kg/m^3.

Silicate component (SC): sodium metasilicate crystalline hydrate $Na_2SiO_3 \cdot 5H_2O$, mass fraction of SiO_2 within 27 - 29%, mass fraction of Na_2O within 28-30%, mass fraction of iron (Fe_2O_3) not exceeding 0.01%, CAS number 10213-79-3 (TU 2145-001-52257004-2002). Its particle size was 0.9-1.25 mm. There are also impurities of calcium and sodium chlorides in the amount of 4-8%.

Preparation of composites

The thermal insulation composite material was produced by free foaming of the reactive mixture components. The component ratio was kept constant for all reactive compositions at IC:PC = 1.8:1. For modification, the silicate component was introduced into the mixture in amounts of 15, 30, 45, 60, 75, and 90 wt% relative to the reactive composition for producing rigid pour-in-place polyurethane foam. The components of the reactive composition were stirred for 30 s at a rotational speed of 1500 rpm. The prepared mixture was poured into a mold and cured for 24 h at a temperature of 22±3 ℃.

Characterization

Infrared spectra of the obtained samples were recorded using an InfraLYUM FT-08 FT-IR spectrometer (Lumex, Russia) equipped with a Quest ATR accessory (Specac, UK) for measurements in the attenuated total reflectance (ATR) mode over the wavenumber range of 400-4000 cm^{-1}.

Thermal tests were performed on an SDT-Q-600 V20.9 Build 20 thermal analyzer in an air atmosphere at a constant heating rate of 20 ℃/min. The measurement results were processed using the supplied TA Universal Analysis software package.

Flammability characteristics were determined using a device for the «experimental determination of flammability of solid substances and materials» (Patent RU No. 243 729). The combustion chamber was made of a steel cylinder with a diameter of 50 mm and a height of 160 mm. An alcohol burner was used as the flame source. The flame height was set to 40 mm. The distance from the combustion chamber to the top edge of the alcohol burner was 20 mm. The test specimens protruded from the lower edge of the combustion chamber by 5 mm. The specimen dimensions were: width 35 mm, height 10 mm, length 150 mm. The exposure time was 60 s.

The limiting oxygen index (LOI) was determined in accordance with GOST 12.1.044-89, clause 4.14.

The structural features of the samples were examined by optical microscopy.

3. RESULTS AND DISCUSSION

To confirm the interaction of isocyanate functional groups with the silicate component (SC), a composite was prepared by mixing these components in a mold (3×2×2 cm) at room temperature without catalysts. 5-10 minutes after the start of mixing, the formation of gas bubbles on the surface was observed (Fig. 1).

Also, air-cured IC was obtained. Analysis of the micrographs of the composite and the air-cured IC reveals differences in color and the formation of pore inclusions in the composite (Fig. 3), in contrast to the dense structure of the crystallized IC (Fig. 2).

Presumably, the interaction between IC and SC should involve a chemical reaction of isocyanate with the crystal hydrate water of the pentahydrate, following the chemical reactions typical of the interaction of isocyanate with aqueous sodium silicate solutions, including the formation of an organomineral compound with a Si-O-C structure [6].

Fig. 1. Photograph of the mixture based on IC and SC 10 min after mixing.

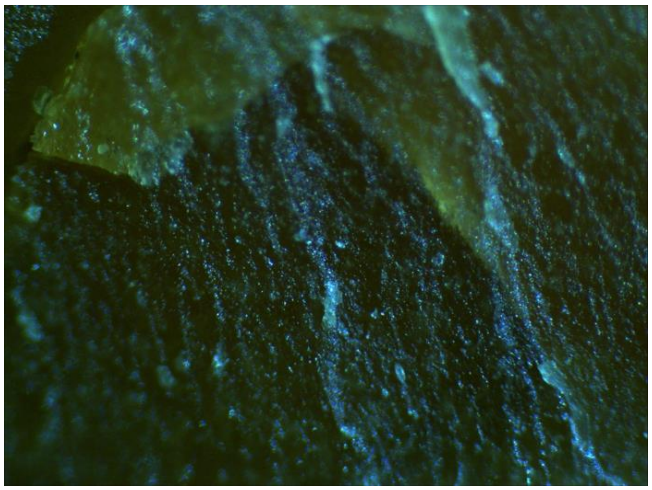

Fig. 2. Micrograph of air-cured IC.

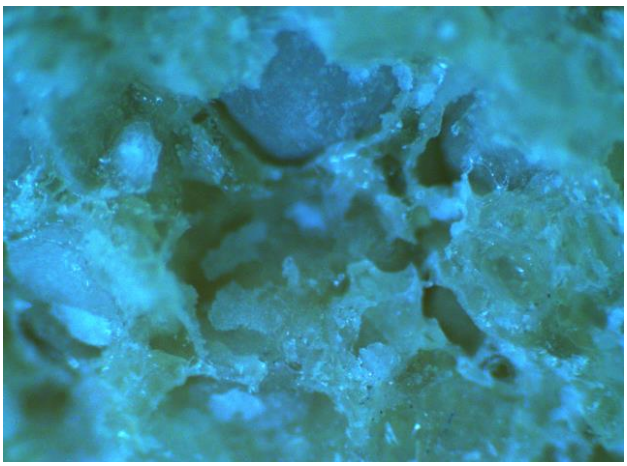

Fig. 3. Micrograph of the cured composite based on IC and SC.

To determine the reactivity of the SC and its influence on the chemical interaction of the components in the PUF mixture, infrared spectra were recorded for:

- Air-cured IC (MDI)
- Sodium metasilicate pentahydrate $Na_2SiO_3 \cdot 5H_2O$
- Composite based on IC and SC
- Control unmodified PUF composition
- PUF composition with 90% SC.

From the analysis of the transmittance spectra of the air-cured IC sample (MDI) (Fig. 4), first of all, a characteristic peak was identified in the region of ~2270 cm^{-1}, which is attributed to isocyanate functional groups -N=C=O. The curing process is considered complete when this band disappears [7, 8].

A broad shoulder from 3150 cm^{-1} to 3450 cm^{-1} with a peak at ~3350 cm^{-1} was detected and assigned to stretching vibrations of (N-H) bonds in urea segments involved in strong intermolecular hydrogen bonding [9].

The transmittance peaks in the wavenumber regions around ~3030 cm^{-1}, ~2835 cm^{-1}, and ~2900 cm^{-1} were assigned to vibrations of carbon-hydrogen bonds in benzene rings and in the central methylene bridge (-CH_2-) [10, 11].

A minor peak at a wavenumber of ~1780 cm^{-1} was attributed to C=O bond vibrations and serves as a marker of four-membered uretdione rings (aromatic dimers) that dissociate upon heating to 130-160 °C [12].

The transmittance peak at a wavenumber of ~1640 cm^{-1} was assigned to stretching vibrations of the carbonyl group (C=O) in urea moieties [13, 14].

The intense transmittance peak at a wavenumber of ~1595 cm^{-1} was assigned to stretching vibrations of C=C bonds in the aromatic (benzene) ring of MDI [15].

The intense transmittance peak at a wavenumber of ~1505 cm^{-1} was assigned to a complex overlap of aromatic ring (C-C) vibrations typical of MDI, along with Amide II, bending vibrations of the (N-H) bond, and stretching vibrations of the (C-N) bond [16-18].

The transmittance peak at a wavenumber of ~1410 cm^{-1} was assigned to bending vibrations of (C-H) bonds in the aromatic rings of MDI with a small contribution from (C-N) bonds of uretdione dimers (the presence of which is evidenced by the weak peak at 1780 cm^{-1}). No isocyanurates are present in the system, as confirmed by the absence of a peak in the region of 1710 cm^{-1} [19].

The transmittance peaks at wavenumbers of ~1305 cm^{-1}, ~1230 cm^{-1}, and ~1200 cm^{-1} were assigned to Amide III bending vibrations δ(N-H) and stretching vibrations ν(C-N), which, together with the peak at 1640 cm^{-1}, confirms the presence of polyurea linkages [20, 21].

All peaks in the wavenumber range of 400-1200 cm^{-1} were assigned to skeletal and bending vibrations of the parent MDI isocyanate and the structure of its benzene rings [22, 23].

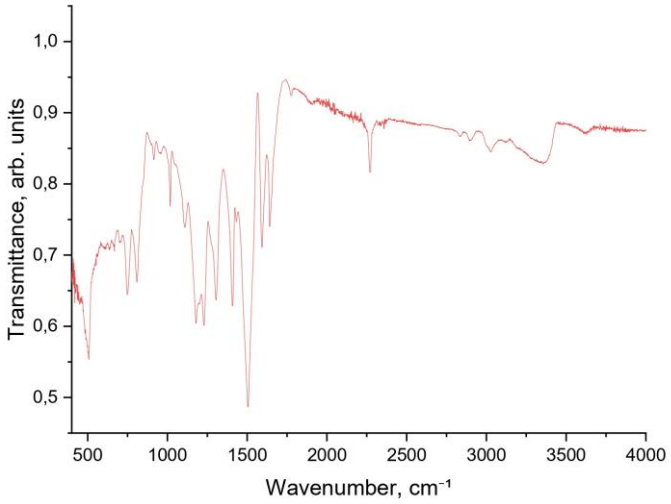

Fig. 4. IR spectra of air-cured MDI.

From the analysis of the transmittance spectra of the sodium metasilicate pentahydrate sample (Fig. 5), the main characteristic peaks were identified: those at ~1120 cm^{-1} and ~830 cm^{-1} were assigned to Si-O-Si vibrations; the peaks in the regions of 970 cm^{-1}, ~880 cm^{-1}, and ~775 cm^{-1} were assigned to Si-OH bond vibrations; and the peak at ~455 cm^{-1} was assigned to O-Si-O bending vibrations. The peak in the region of ~1435 cm^{-1} was attributed to stretching vibrations of the carbonate ion, which could have been caused by partial carbonation during grinding [24-27].

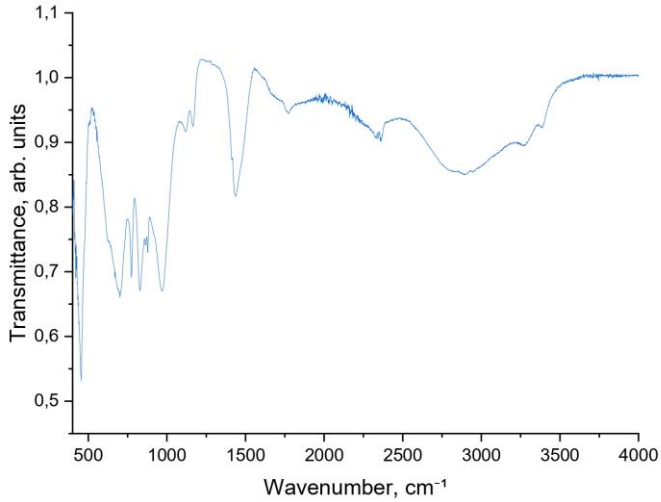

Fig. 5. IR spectra of $Na_2SiO_3 \cdot 5H_2O$ (SC).

To prepare composite samples based on MDI and sodium metasilicate pentahydrate, the latter was preliminarily evacuated to avoid the influence of adsorbed moisture. The transmittance spectra of the sample (Fig. 6) are complex, involving overlap and interaction with crystal hydrate water at the liquid-solid interface, which is confirmed by the formation of polyurea linkages and more efficient consumption of isocyanate groups.

At the same time, no new organomineral Si-O-C bonds with characteristic transmittance bands in the regions of 840 and 1080 cm^{-1} were detected [6].

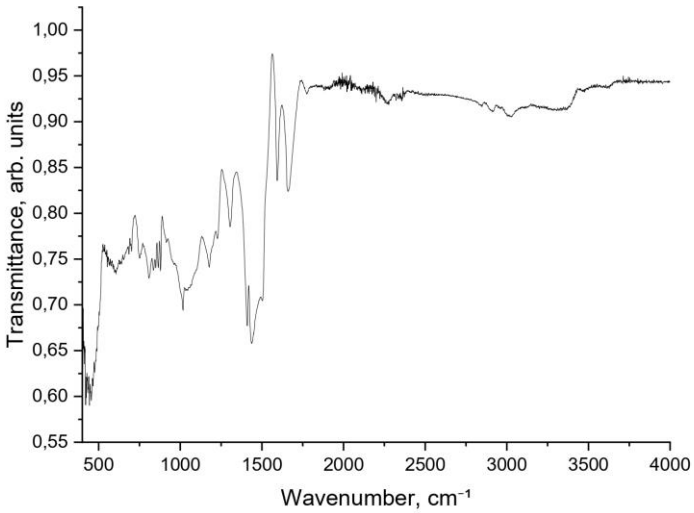

Fig. 6. IR spectra of the air-cured composite based on MDI and SC.

For the quantitative analysis of the degree of conversion of isocyanate groups, the relative degree of conversion of isocyanate groups (X) was calculated from the change in the normalized optical density of the asymmetric stretching vibration band of the NCO group (2270 cm^{-1}). The stretching vibration band of the aromatic skeleton of MDI (1595 cm^{-1}), whose intensity does not change during the polymer curing process, was used as an internal standard [28].

Additionally, in Ref. [29] the authors introduce the relative absorbance (A_i) at a given time as the ratio of the absorbance of the analytical peak at 2270 cm^{-1} to that of the peak at 2869 cm^{-1}, chosen as a reference value and not involved in the cyclic trimerization reaction ($A_i = A_{2270}/A_{2869}$). The kinetics and the extent of conversion were evaluated through the change in the ratio of the current index to the initial one: (A_i/A_0).

Accordingly, the transmittance in arbitrary units from 0 to 1 was converted to absorbance using formula (1):

$$A = -\log_{10}(T) \quad (1)$$

The relative absorbance was determined by formula (2):

$$A_i = A_{2270}/A_{1595} \quad (2)$$

The relative degree of conversion of isocyanate groups, Δ(X), was determined by formula (3):

$$\Delta X = (1 - A_{i1}/A_{i2}) \cdot 100 \quad (3)$$

From the calculations, the relative absorbance for the composite sample based on MDI and pentahydrate (A_{i1}) was 0.51, and for the air-cured MDI (A_{i2}) it was 0.62. The relative amount of remaining NCO groups in the MDI sample is larger; therefore, the composite is «more cured». If the MDI sample is taken as a conventional reference point, the isocyanate conversion in the second sample is ~22% higher.

Analysis of the spectra of the control PUF composition confirmed the predominance of urethane compounds; however, it was not possible to identify polyurea linkages due to the complex nature and overlap of the transmittance bands, which indicates their insignificant amount. Analysis of the spectra of the PUF composition with 90% SC showed that, similarly to the composite based on MDI and pentahydrate, the transmittance bands exhibited a complex pattern of overlapping bands, and no new compounds were detected.

To determine the fire-retardant mechanism of the SC and to assess its influence on the thermal properties of the composite, TG and DTG analyses of the thermo-oxidative degradation of the SC, the control PUF composition, and PUF with 90% SC were performed.

From the analysis of the TG and DTG curves of sodium metasilicate pentahydrate (Fig. 7), it can be seen that the mass loss of the sample begins at 54 °C, corresponding to the evaporation of surface-adsorbed moisture. The melting point is 72 °C (intersection of the tangents to the TG curve). At this temperature, the sample loses ~1 % of its mass. According to the DTG curve, the decomposition rate in this region increases to an extremum point at 79 °C, reaching 0.31 %/°C. Subsequently. the decomposition rate decreases and reaches a new peak at 100 °C, at which point the sample mass is 91.2 %. The portion of the curve from 72 to 100 °C can be tentatively attributed to the evaporation of the first water molecule.

Then the rate decreases to an extremum point at 122.3 °C, reaching 0.13 %/°C, at which time the sample mass is 86.2 %. Afterwards, the rate increases to 0.5 %/°C at 137 °C, and at the point of intersection of the tangents to the DTG curve in this region (134 °C) the sample mass is 83 %, which corresponds to the loss of two water molecules.

Subsequently, the rate slightly decreases to 0.41 %/°C at 149 °C and then increases to a maximum at 163 °C, reaching 0.88 %/°C. The intersection of the tangents to the DTG curve at the lower part and the rising part corresponds to 153 °C, at which the sample mass is 74.4 %, allowing the temperature range from 134 to 153 °C to be assigned to the loss of the third water molecule.

After that, the rate drops sharply to 0.12 %/°C at 172 °C, followed by a monotonic decrease to near-zero values and reaching a plateau. The tangents to the maximum of the DTG curve and to the subsequent descending part intersect at 164.7 °C, where the sample mass is 65.9 %. Accordingly, the

temperature interval from 153 to 164,7 ℃ can be attributed to the evaporation of the fourth water molecule.

The monotonic decrease in the decomposition rate continues down to 254 ℃, with a slight rise to an extremum point of 0.022 %/℃ at 260 ℃, and then decreases to near-zero values at 265 ℃. At the starting point of this rise (254 ℃), the sample mass is 61.8 %; thus, in the range from 164.7 to 254 ℃, 0.5 water molecules are evaporated. Thereafter, the sample mass slowly and monotonically decreases to 60.8 % at 400 ℃ and remains constant upon further heating.

Thus, the fire-retardant mechanism of the pentahydrate upon heating consists of the intense release of crystallization water as vapor in the temperature range of ~70 to ~170 ℃, which leads to phlegmatization, dilution of the gas-phase combustion zone with displacement of oxygen, and absorption of thermal energy. Moreover, the intense transition of crystallization water to vapor, with a volume increase of up to 1700 times, causes intumescence of the metasilicate, which forms a highly porous heat-insulating barrier and, through additional thermal resistance, impedes further degradation of the material.

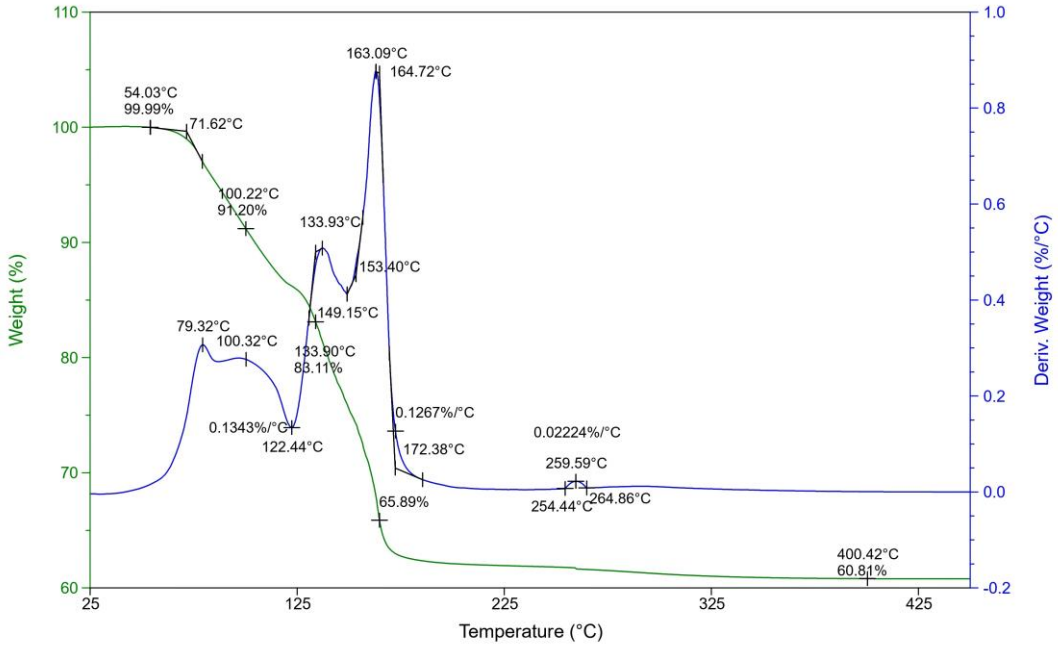

Fig. 7. TG and DTG curves of $Na_2SiO_3 \cdot 5H_2O$ in an air atmosphere.

To evaluate the thermo-oxidative stability of the control polyurethane foam sample, investigations were carried out in the presence of atmospheric oxygen, which leads to a multistage degradation process (Fig. 8) [30, 31].

The thermal stability of the sample under thermo-oxidative degradation is lower than under pyrolysis, and the overall degradation reactions occur at temperatures 30-70 ℃ lower than in an inert atmosphere. This is explained by the oxidizing ability of oxygen, which actively participates in initiating free-radical reactions, forming peroxide radicals, and subsequently yielding unstable hydroperoxides through chain reactions [32, 33].

From the IR analysis, it is known that the control composition contains only urethane and urea segments, namely aromatic urethane and disubstituted urea. Based on the knowledge of the thermal stability of these groups, it is known that the onset temperature of thermal dissociation for them is in the range of 180-200 ℃ and 200-250 ℃, respectively [34].

On the TG curve, the sample remains stable up to 170 ℃, indicating the absence of adsorbed moisture, and the onset temperature of mass loss can be attributed to the beginning of urethane group decomposition [35, 36]. It has also been noted in [37] that the use of triethylenediamine as a catalyst initiates early thermo-oxidative degradation of urethanes at a temperature of about 170-180 ℃,

whereas in [6] the onset temperature of thermal decomposition of PUF in an N_2 atmosphere was reported to be approximately 200-220 ℃.

Upon further heating, a gradual mass loss of 5 % is observed up to 273 ℃, with minor DTG peaks at 204 and 220 ℃, which can be attributed to the onset of decomposition of polyurea segments [34]. The primary decomposition pathway of these bonds is associated with thermal dissociation and represents a reversible reaction-dissociation into their constituents: for urethanes, into isocyanate and polyol; for ureas, into isocyanate and amine group.

Further heating accelerates these processes, which are accompanied by consecutive recombination with the formation of new compounds, including volatile gaseous products, accounting for a 33 % mass loss in the range from ~270 to ~370 ℃, with a DTG peak at 320 ℃ corresponding to a rate of 0.67 %/℃. This region can be assigned to the decomposition of isocyanates. Thus, in [38] a rapid loss of isocyanate in the heating range of 200-300 ℃ was noted, with the formation of a characteristic yellow smoke attributed to a mixture of nitrogen-containing hydrocarbons such as hydrogen cyanide, acetonitrile, acrylonitrile, pyridine, and benzonitrile. Also, in [39] the first stage corresponding to 32-34 % mass loss was assigned to the loss of nitrogen-containing fragments. In [40], the first stage of thermal degradation of polyurea was characterized by a DTG peak at 322 ℃ and was likewise attributed to the degradation of the hard segment.

The subsequent shoulder from ~370 ℃ to ~500 ℃, with a DTG extremum at 412 ℃ and a rate of 0.06 %/℃, is characterized by a mass loss of 11 % and is associated with the decomposition of secondary, more thermally stable compounds [41].

Furthermore, in [42] the release of HCN at a temperature of about 365 ℃ and the release of CO_2 occurring in two stages-in the ranges of 220-450 ℃ and 550-650 ℃, respectively-were discussed.

The next main stage of degradation is characterized by a 43 % mass loss in the temperature range from 495 to 640 ℃, with a maximum decomposition rate of 0.48 %/℃ at 555 ℃. This region should be attributed to the further decomposition of previously formed compounds, as well as to the subsequent radical cleavage of the polyol chain, detachment, and rearrangement of simple radicals, resulting in the formation of gaseous substances. Thus, in [43], heating PUF from 400 to 800 ℃ led to the formation of methane, ethene, ethane, propane, ethanal, and propanal in various concentrations, with methane formation peaking at 600 ℃.

The following shoulder in the range of 640-690 ℃ is associated with the oxidative combustion of the carbonaceous residue formed in the previous stages of polymer degradation. At these temperatures, carbon is oxidized to CO and CO_2, which completes the mass loss to a minimum at 690 ℃, leaving a carbon residue of 3.6 %.

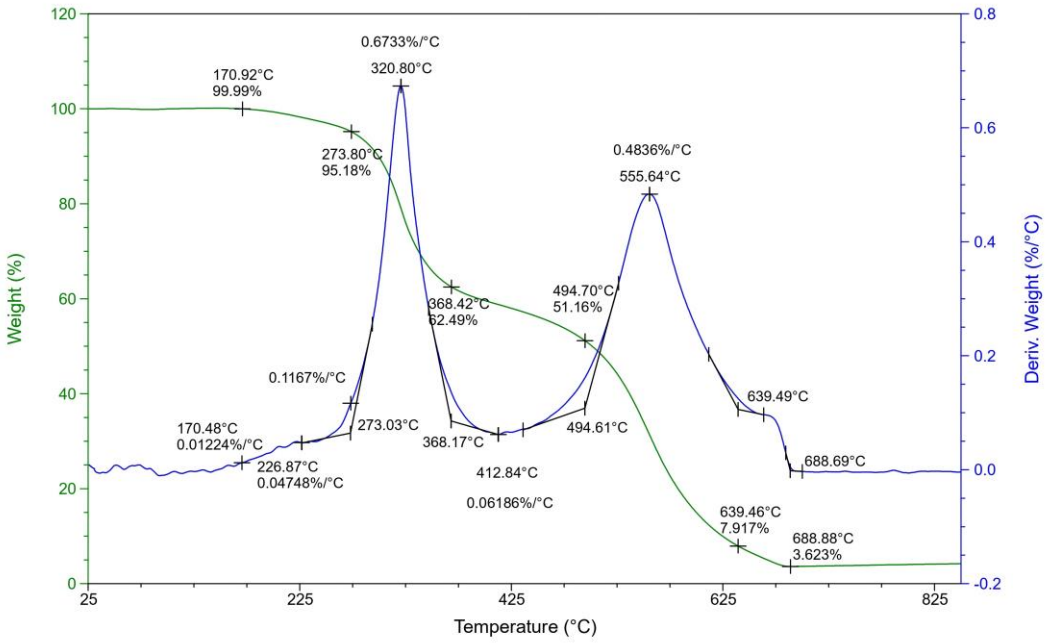

Fig. 8. TG and DTG curves of the control PUF composition in an air atmosphere.

To investigate the effect of filling polyurethane foam with sodium metasilicate pentahydrate on the thermo-oxidative stability of the composites, a sample filled with 90% SC of the 0.9-1.25 mm fraction was studied (Fig. 9).

Based on the results of the IR spectral analysis of this composition, where it was concluded that there are no clear signs of chemical interaction with the formation of C-N-O organomineral bonds, it can be assumed that upon heating the majority of the chemically bound water will evaporate. The final residue of the sample will contain dehydrated sodium metasilicate (57.5 wt% of the initial pentahydrate mass) and the carbonaceous residue of PUF (3.62 wt% of the initial polymer matrix mass), which, in the absence of stable organomineral compounds formed through secondary reactions, would theoretically amount to 28.93 wt% of the composite.

From the analysis of the DTG curve of the thermo-oxidative degradation of the sample, a monotonic slight increase in the rate is observed up to 72-79 ℃; this region can be attributed to the evaporation of unbound adsorbed moisture. Then the rate increases up to 120 ℃, where it rises sharply to 134 ℃. This region correlates with the previously obtained data for the initial pentahydrate, where a lower extremum at 122 ℃ with a subsequent sharp rise to 137 ℃ was observed, and at 134 ℃ the evaporation of two water molecules tentatively occurs. Subsequently, the rate decreases up to 190 ℃ and ends with a minimum point at 205 ℃, followed by a monotonic increase. At the same time, at 190 ℃ on the TG curve, the sample is characterized by a loss of ~18%, which can be conditionally attributed to the loss of ~4.5 water molecules of sodium metasilicate pentahydrate, which directly correlates with the pattern of thermo-oxidative degradation of the latter in its pure form. The minimum point on the DTG curve at this temperature is reflected in the DTG curve of the control sample, where a minor peak was noted at 204 ℃. The subsequent monotonic decomposition correlates with the control composition and can also be attributed to the thermal dissociation of urethane and urea segments. An extreme increase in the decomposition rate begins from 254 ℃ at a rate of 0.1 %/℃ to 295 ℃ at a rate of 0.42 %/℃, followed by a decline to 0.06 %/℃ at 353 ℃ and is characterized by a 20 wt% mass loss of the sample, which, when recalculated for the loss of the organic component, amounts to ~38% and, on the whole, correlates with the mass loss for the first main stage of the control composition.

The shift of the thermo-oxidative degradation to lower temperatures - the peak shifts from 320 to 295 ℃ - may be associated with the catalytic effect of sodium alkali metal ions on the decomposition of urethane and urea bonds [44, 45]. Metal ions can accelerate the decomposition process through the formation of coordination bonds between the metal cation and the functional groups of the polymer (e.g., with the heteroatoms of oxygen and nitrogen in urethane and urea groups) [46], which leads to a shift of electron density from the heteroatom to the cation and weakening of adjacent bonds in the polymer backbone, thereby facilitating bond cleavage and reducing the activation energy of the degradation process [47-50]. The alkaline nature of sodium promotes the acceleration of thermal decomposition [51], and the release of water at the initial stage can contribute to the alkaline hydrolysis of urethane and urea bonds and lead to their dissociation [52].

The subsequent shoulder of the DTG curve from 353 to 452 ℃ is characterized by a loss of 5 wt%, which, recalculated for the organic part, amounts to ~10% and also correlates with the results for the control composition.

The second main stage of the organic matrix decomposition, from 353 to 555 ℃, with a peak at 522 ℃ and a rate of 0.28 %/℃, shows a shift of the onset and the end by 42 and 85 ℃, and the peak by 33 ℃ to lower temperatures, and is characterized by a loss of 20 wt%, which, recalculated for the organic part, amounts to 38%.

The following shoulder from 555 to 600 ℃ is similar in nature to that of the control composition, with a shift of the onset and the end by 85 and 90 ℃, reaching a residual mass of 29%, which directly correlates with the theoretical calculation, thereby confirming the absence of the formation of new, more thermally stable organomineral compounds.

Thus, the composite is characterized by three main stages of decomposition, where:

1 – decomposition of the pentahydrate with the release of crystal hydrate water;

2 – dissociation of urethane and polyurea bonds with their subsequent chain recombination, as well as decomposition of MDI;

3 – decomposition of the polyether component and of the compounds formed during the preceding chain reactions.

Herewith, sodium metasilicate pentahydrate does not fundamentally alter the decomposition pattern but leads to a shift of the reactions toward lower temperatures due to the catalytic effect.

From the analysis of the data obtained (Tables 1-2), it can be concluded that for the second main decomposition region, compared to the analogous region of the control composition, the onset temperature shifted to lower temperatures from 270 to 255 ℃ by 15 ℃, the end temperature from 370 to 350 ℃ by 20 ℃, the mass loss decreased from 33 to 20 wt% by 39%, the DTG peak temperature decreased from 320 to 295 ℃ by 25 ℃, the mass loss rate decreased from 0.67 to 0.42 %/℃ by 37%, and the maximum heat flow decreased from 8 to 5.4 W/g by 33%.

For the third main decomposition region, compared to the analogous region of the control composition, the onset temperature shifted to lower temperatures from 495 to 450 ℃ by 45 ℃, the end temperature from 640 to 555 ℃ by 85 ℃, the mass loss decreased from 43 to 20 wt% by 53%, the DTG peak temperature decreased from 555 to 520 ℃ by 35 ℃, the mass loss rate decreased from 0.48 to 0.28 %/℃ by 42%, and the maximum heat flow decreased from 18.8 to 7.7 W/g by 59%.

The end temperature of decomposition decreased from 690 to 600 ℃ by 90 ℃, while the final char residue increased from 3.6 to 29.1 wt% by a factor of 8.1.

Table 1. Thermal properties of unmodified PUF.

Composition name	Control PUF composition						
Parameter name	№	Temperature, ℃		Mass loss, wt%	DTG peak temperature, ℃	Mass loss rate, %/℃	Maximum heat flow, W/g
		Onset	End				
Main decomposition stages	1	270	370	33	320	0.67	8.0
	2	495	640	43	555	0.48	18.8

Table 2. Thermal properties of the PUF composition with 90% SC, 0.9–1.25 mm fraction.

Composition name	PUF composition with 90% SC, 0.9–1.25 mm fraction						
Parameter name	№	Temperature, ℃		Mass loss, wt%	DTG peak temperature, ℃	Mass loss rate, %/℃	Maximum heat flow, W/g
		Onset	End				
Main decomposition stages	1	80	205	18	135	0.3	1.4
	2	255	350	20	295	0.42	5.4
	3	450	555	20	520	0.28	7.7

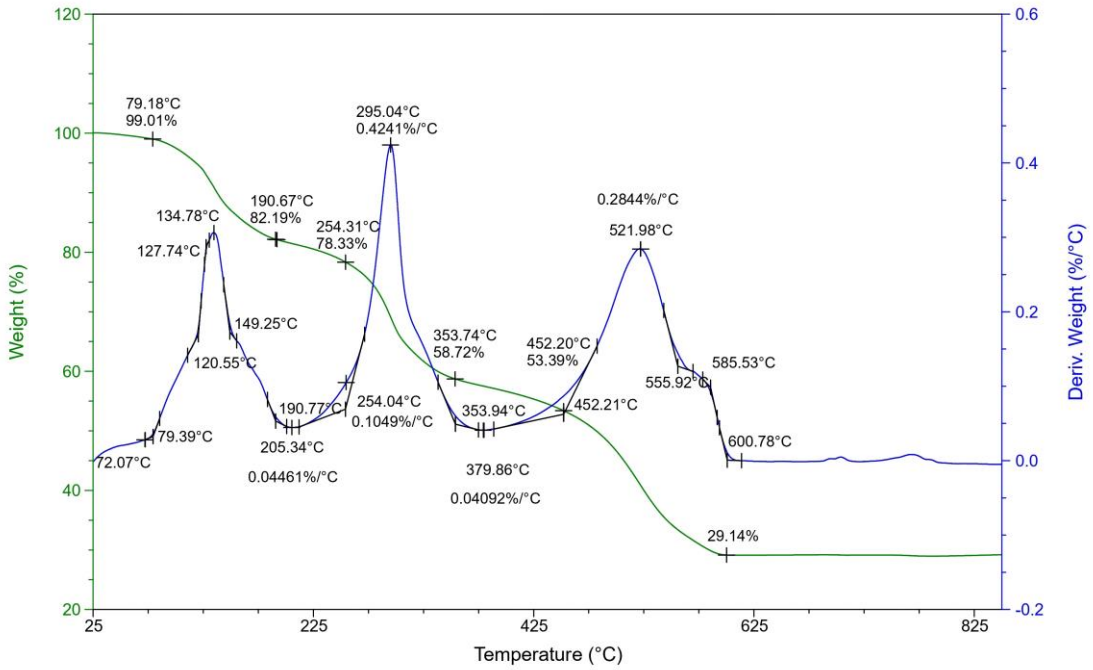

Fig. 9. TG and DTG curves of the PUF composite composition with 90% SC in an air atmosphere.

Previously, to assess the flammability of composites with the SC of the 0.9-1.25 mm fraction, tests were carried out according to the UL-94 (Standard for Safety of Flammability of Plastic Materials for Parts in Devices and Appliances) vertical burning test [5]. According to the results, the control sample and the modified sample with 15% SC failed the test and therefore could not be assigned a rating. The sample with 30% SC achieved a V-1 rating, and the following samples with a silicate component content of 45-90% achieved the highest rating of V-0.

For a more detailed study of the effect on flammability, tests were conducted on a custom-developed device (Pat. RU 243 729). The results of the extent of damage along the length of the samples are presented in Fig. 10. It can be seen from the figure that, although a fire-retardant intumescent layer is formed from the SC, its coating density is insufficient to prevent damage along the length; the damage, however, is superficial in nature, which can be seen in the cross-section of the material in Fig. 11 and is also confirmed by a significant reduction in the degree of damage by mass – down to 15% at an SC concentration of 90%, compared to 82% damage for the control composition (Fig. 12).

A schematic illustration of the fire-retardant mechanism is presented in Fig. 13.

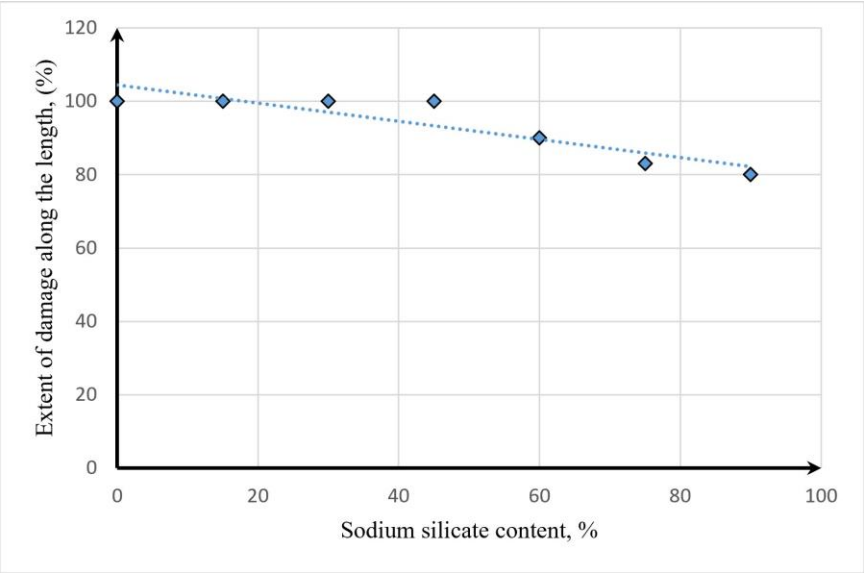

Fig. 10. Dependence of the change in the extent of damage along the length (%) of the composite samples on the SC content, 0.9-1.25 mm fraction.

Fig. 11. Photograph of a cross-section of the composite sample after fire tests, composition with 90% SC, 0.9-1.25 mm fraction.

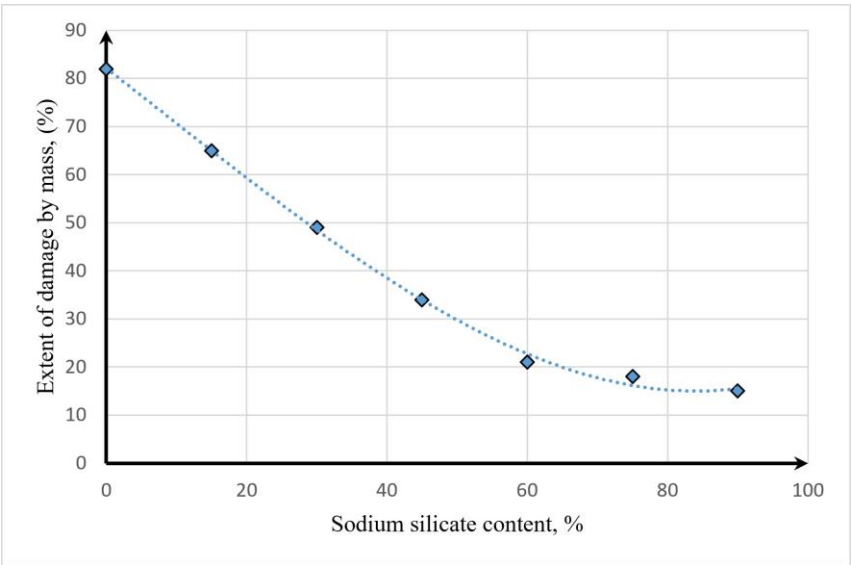

Fig. 12. Dependence of the change in the extent of damage by mass (%) of the composite samples on the SC content, 0.9-1.25 mm fraction.

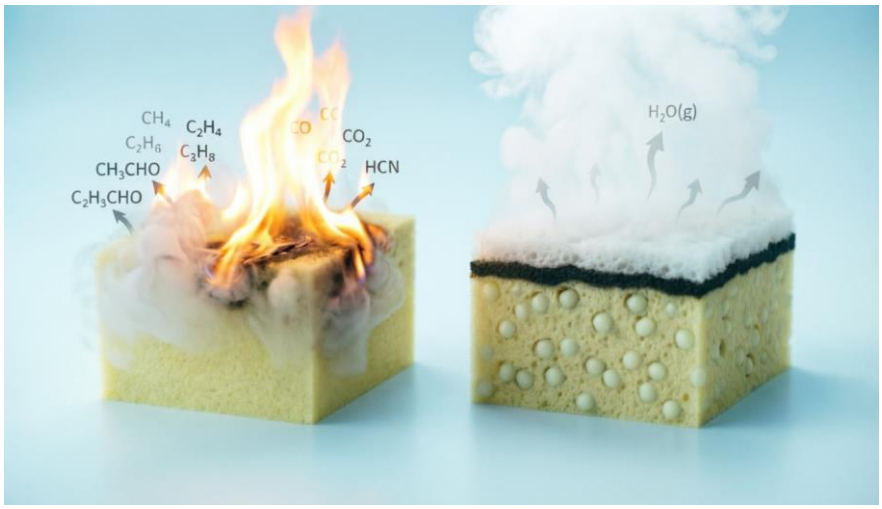

Fig. 13. The fire-retardant mechanism of the silicate component.

To evaluate the fire-retardant effect of the SC, temperatures inside the material and the temperature of the exhaust flue gases were measured zone-by-zone. The temperature change curves for the control sample and the samples with SC concentrations of 60% and 90% are presented in Fig. 14, Fig. 15, and Fig. 16, respectively, where 1 – temperature values in the "bulk" of the material at a distance of 1/3 L from the edge of the sample, 2 – temperature values in the "bulk" of the material at a distance of 2/3 L from the edge of the sample, 3 – temperature values of the exhaust flue gases.

The control composition was characterized by instantaneous ignition, as a result of which the exhaust flue gas curve rises sharply. The temperature inside the material at a distance of 1/3 of the sample length from the edge reaches a maximum of ~320 °C already after ~20 s from the start of the test and then decreases; this coincides with the DTG peak temperature of the first decomposition stage of the control composition. The temperature inside the material at a distance of 2/3 of the sample length from the edge begins to increase rapidly after ~15 s from the start, at the moment when the temperature in the lower zone reaches ~200 °C, which also coincides with the onset of PUF decomposition according to the DTG curve. The maximum temperature here amounts to ~360 °C after 25 s and then drops until complete burnout, which occurred after 38 s from the start of the test. The subsequent dashed curve represents the inertial cooling of the thermocouple.

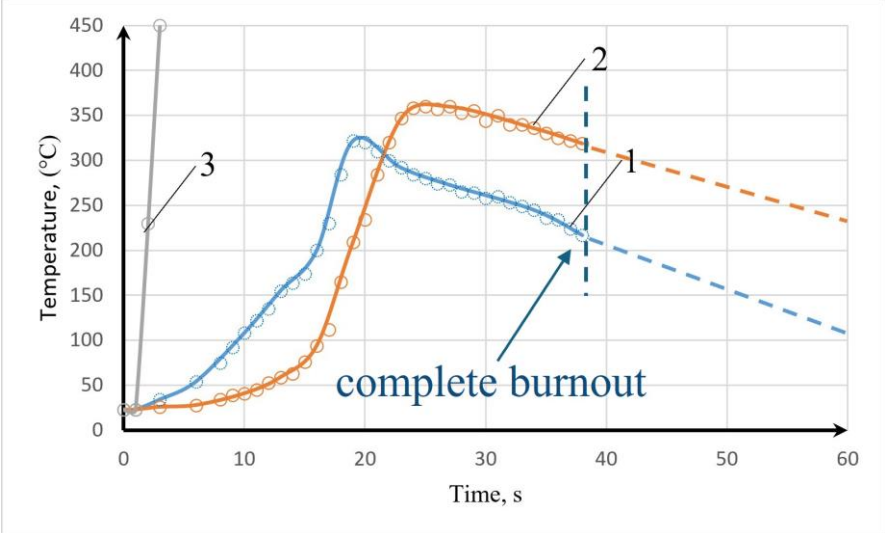

Fig. 14. Temperature changes over time (s) within the material and in the exhaust flue gases for the control unmodified PUF composition.

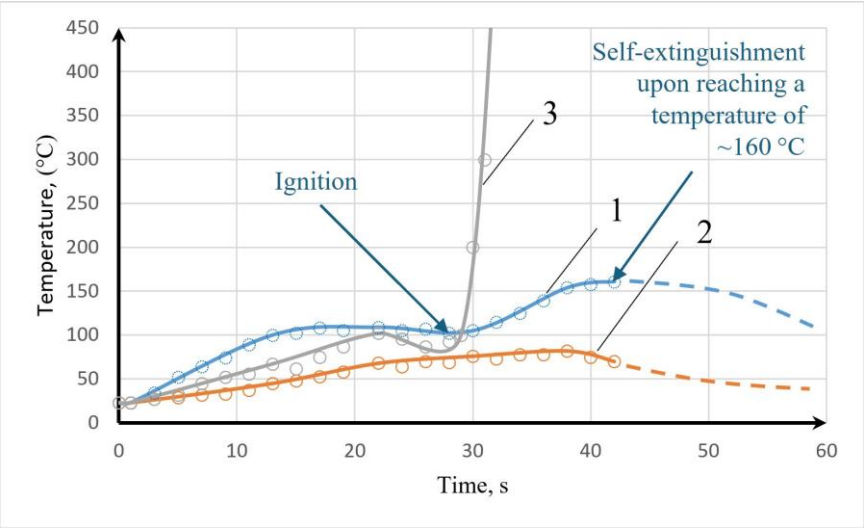

Fig. 15. Temperature change over time (s) within the material and in the exhaust flue gases for the PUF composite composition with 60% SC, 0.9-1.25 mm fraction.

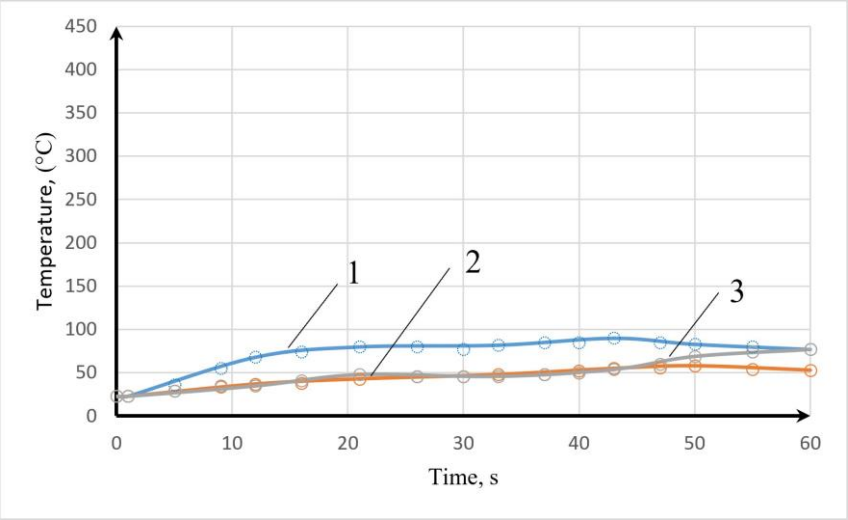

Fig. 16. Temperature change over time (s) within the material and in the exhaust flue gases for the PUF composition with 90% SC, 0.9-1.25 mm fraction.

Also, to assess flammability, the limiting oxygen index (LOI) was determined for the control composition and for the sample with the best performance in the previous stages, at a concentration of 90%. The test results were 17.8 and 26.6, respectively, which allows this polyurethane foam matrix composite material to be classified as self-extinguishing and moderately combustible materials [53-55].

4. CONCLUSIONS

From the analysis of the totality of the test results for the composites modified with the silicate component, it can be concluded that the resulting three-dimensional heterophase cellular structure is provided by the chemical interaction of the isocyanate functional groups of the reactive mixture with the water of the SC at the phase boundary, without the formation of new organomineral compounds.

The fire-retardant mechanism of the SC upon heating consists of the intense release of crystallization water as vapor in the temperature range of ~70 to ~170 °C, which leads to phlegmatization, dilution of the gas-phase combustion zone with displacement of oxygen, and absorption of thermal energy. At the same time, the intense transition of crystallization water to vapor, with a volume increase, causes intumescence of the metasilicate, which forms a highly porous heat-insulating barrier and, through additional thermal resistance, impedes further degradation of the material. The SC does not fundamentally alter the decomposition pattern but shifts the reactions to lower temperatures (by 15-85 °C) owing to the catalytic effect of sodium alkali metal ions. The residue after thermo-oxidative degradation increases in direct proportion to the amount of the introduced SC, corresponding to its dehydrated part (Na_2SiO_3).

UL-94 tests and tests on the custom-developed device (Pat. RU 243 729) showed that at an SC loading of 45-90%, the material achieves a V-0 rating and a reduction in the extent of damage by mass from 82% to 15-34 wt% compared to the control, while at 90% SC the oxygen index increases from 17.8 to 26.6 compared to the control, which places the material in the category of self-extinguishing, moderately combustible materials and makes it possible to recommend the use of sodium metasilicate crystalline hydrates to reduce the flammability of composites based on other polymer matrices.

5. ACKNOWLEDGEMENTS

The work was carried out at NIU MSCU within the framework of the University Development Program “PRIORITY 2030”. Project 3.1 “Scientific breakthrough in the construction industry - new technologies, new materials, new methods”.
The research was funded by the National Research Moscow State University of Civil Engineering (grant for fundamental scientific research, project No. 04-482/130).

REFERENCES

1. Kairytė A., Makowska S., Rybiński P., Strzelec K., Kremensas A., Šeputytė-Jucikė J., Vaitkus S. Effect of Liquid Glass-Modified Lignin Waste on the Flammability Properties of Biopolyurethane Foam Composites. Polymers. 2024. 16 (2). P. 205. DOI: 10.3390/polym16020205
2. Feng J. et al. A Si-containing polyphosphoramide via green chemistry for fire-retardant polylactide with well-preserved mechanical and transparent properties. Chemical Engineering Journal. 2022. 431. P. 134259.
3. Pustovgar A.P., Bruyako M.G., Petunova M.D. et al. Hybrid materials based on Na-liquid glass, 2,4-toluene diisocyanate, epoxy oligomer and polyisocyanate. Polymer Science. Series A. 2018. 60 (6). P. 495 – 512. DOI: 10.1134/S230811201806007X
4. Lipka P.A., Mironova K.A., Bruyako M.G., Kozlova I.V., Samchenko S.V. Organomineral thermal insulation composite: pore structure formation. Technique and Technology of Silicates. 2026. 33 (1). P. 46 – 59. DOI: 10.62980/2076-0655-2026-46-59
5. Lipka P.A., Borisenkov N.S., Mironova K.A., Chesnokova D.S., Bruyako M.G. Thermal insulation composite material based on sodium silicate and polyurethane foam matrix. Technique and Technology of Silicates. 2026. 33 (2). P. 154 – 166. DOI: 10.62980/2076-0655-2026-154-166
6. Ishchenko S.S., Pridatko A.B., Novikova T.I., Lebedev E.V. Interaction of isocyanates with aqueous solutions of alkali metal silicates. Polymer Science. Series A. 1996. 38 (5). P. 786 – 791.
7. Kozakiewicz J., Rokicki G., Przybylski J., Pawłowski P. Water-cured poly(urethane-urea)s containing soft segments originating from siloxane/carbonate macrodiols. Polimery. 2012. 57 (11-12). P. 791 – 798. DOI: 10.14314/polimery.2012.791
8. Chemical Encyclopedia. ed. by I.L. Knunyants. Moscow.1990. 5 (2). P. 671.

9. Bugrov A.N., Gorshkova Y.E., Ivan'kova E.M., Kopitsa G.P., Pavlova A.A., Popova E.N., Smirnova V.E., Smyslov R.Y., Svetlichnyi V.M., Vaganov G.V., Vasil'ev B.V. Domain Structure, Thermal and Mechanical Properties of Polycaprolactone-Based Multiblock Polyurethane-Ureas under Control of Hard and Soft Segment Lengths. Polymers. 2022. 14 (19). P. 4145. DOI: 10.3390/polym14194145
10. Stanciu I. Study of the composition of aromatic hydrocarbons using IR spectroscopy. International Journal of Advanced Scientific Research. 2025. 10 (4). P. 138 – 139.
11. Kobelev A.A., Naganovskii Yu.K., Kruglov E.Yu., Aseeva R.M., Shapikhov E.M. Pyrolysis of hybrid polyurethane-inorganic thermal insulation: thermogravimetric analysis and FT-IR spectra. Fire and Explosion Safety. 2022. 31 (4) P. 5 – 15. DOI: 10.22227/0869-7493.2022.31.04.5-15
12. Sandjong Kuigwa L. Recherche de nouveaux solvants éco-compatibles de substitution dans le cadre de REACH. PhD thesis in Chemistry. Lyon : Université Claude Bernard – Lyon I, 2013.
13. Mel'nik I.V., Lyashenko O.V., Zub Yu.L., Chuiko A.A., Cauzzi D., Predieri G. Synthesis of alkoxysilanes as starting substances for preparation of new materials by the sol-gel procedure. Silanes with urea functional group. Russian Journal of General Chemistry. 2004. 74 (11). P. 1658 – 1664. DOI: 10.1007/s11176-005-0080-x
14. Zhuang Y., Fang Z., Yuan Z., Luo Q., Xu W. Study on the influence of raw material dosages on the production temperature of flexible polyurethane foam. Journal of Polymer Research. 2025. 32 (5). P. 181. DOI: 10.1007/s10965-025-04409-w
15. Stanciu I. Study of the composition of aromatic hydrocarbons using IR spectroscopy. International Journal of Advanced Scientific Research. 2025. 10 (4). P. 138 – 139.
16. Mandal K.K. Infrared Spectroscopy. SEM-4. CC-8. 6. PPT-12. Kolkata : St. Paul's C. M. College, [s. a.]. P 4.
17. Gu X.H., Sung L.-P., Kidah B., Oudina M., Clerici C., Hu H. Q., Stanley D., Byrd W.E., Jean J.Y.C., Nguyen T., Martin J.W. Multiscale physical characterization of an outdoor-exposed polymeric coating system. Journal of Coatings Technology and Research. 2009. 6 (1). P. 67 – 79. DOI: 10.1007/s11998-008-9108-6
18. Duong L.D., Nam G.-Y., Oh J.-S., Park I.-K., Luong N.D., Yoon H.-K., Lee S.-H., Lee Y., Yun J., Lee C.-G., Hwang S.-H., Nam J.-D. High Molecular-Weight Thermoplastic Polymerization of Kraft Lignin Macromers with Diisocyanate. BioResources. 2014. 9 (2). P. 2359 – 2371. DOI: 10.15376/biores.9.2.2359-2371
19. Reignier J., Méchin F., Sarbu A. Chemical gradients in PIR foams as probed by ATR-FTIR analysis and consequences on fire resistance. Polymer Testing. 2021. 93. P. 106972. DOI: 10.1016/j.polymertesting.2020.106972
20. Stani C., Vaccari L., Mitri E., Birarda G. FTIR investigation of the secondary structure of type I collagen: New insight into the amide III band. Spectrochimica Acta Part A: Molecular and Biomolecular Spectroscopy. 2020. 229. P. 118006. DOI: 10.1016/j.saa.2019.118006
21. Zhang S., Ren Z., He S., Zhu Y., Zhu C. FTIR spectroscopic characterization of polyurethane-urea model hard segments (PUUMHS) based on three diamine chain extenders. Spectrochimica Acta Part A: Molecular and Biomolecular Spectroscopy. 2007. 66 (1). P. 188 – 193. DOI: 10.1016/j.saa.2006.02.041
22. Fug F., Rohe K., Vargas J., Nies C., Springborg M., Possart W. 4,4′-methylene diphenyl diisocyanate – Conformational space, normal vibrations and infrared spectra. Polymer. 2016. 99. P. 671 – 683. DOI: 10.1016/j.polymer.2016.07.075
23. Pitsevich G.A., Shundalau M.B., Ksenofontov M.A., Umreiko D.S. Vibrational analysis of 4,4'-methylene diphenyl diisocyanate. Global Journal of Analytical Chemistry. 2011. 2 (3). P. 114 – 124.
24. Torres-Carrasco M., Palomo J.G., Puertas F. Sodium silicate solutions from dissolution of glass wastes. Statistical analysis. Materiales de Construcción. 2014. 64 (314). P. e014. DOI: 10.3989/mc.2014.05213

25. Salazar Navarro A.A., Valdez Salas B. Synthesis of silica nanoparticles from sodium metasilicate. International Journal of Nanoparticles. 2022. 14 (1). P. 1 – 12. DOI: 10.1504/IJNP.2022.122939
26. Shao Z., Luo F., Cheng X., Zhang Y. Superhydrophobic sodium silicate based silica aerogel prepared by ambient pressure drying. Materials Chemistry and Physics. 2013. 141 (1). P. 570– 575. DOI: 10.1016/j.matchemphys.2013.05.064
27. Yang X., Roonasi P., Holmgren A. A study of sodium silicate in aqueous solution and sorbed by synthetic magnetite using in situ ATR-FTIR spectroscopy. Journal of Colloid and Interface Science. 2008. 328 (1). P. 41 – 47. DOI: 10.1016/j.jcis.2008.08.061
28. Modesti M., Lorenzetti A. An experimental method for evaluating isocyanate conversion and trimer formation in polyisocyanate–polyurethane foams. European Polymer Journal. 2001. 37 (5). P. 949 – 954. DOI: 10.1016/S0014-3057(00)00209-3
29. Li J., Jiang S., Ding L., Wang L. Reaction kinetics and properties of MDI base poly (urethane-isocyanurate) network polymers. Designed Monomers and Polymers. 2021. 24 (1). P. 265 – 273. DOI: 10.1080/15685551.2021.1971858
30. Duquesne S., Le Bras M., Bourbigot S., Delobel R., Camino G., Eling B., Lindsay C., Roels T. Thermal degradation of polyurethane and polyurethane/expandable graphite coatings. Polymer Degradation and Stability. 2001. 74 (3). P. 493 – 499. DOI: 10.1016/S0141-3910(01)00177-X
31. Deng Y., Dewil R., Appels L., Ansart R., Baeyens J., Kang Q. Reviewing the thermo-chemical recycling of waste polyurethane foam. Journal of Environmental Management. 2021. 278 (1). P. 111527. DOI: 10.1016/j.jenvman.2020.111527
32. He J.-J., Jiang L., Sun J.-H., Lo S. Thermal degradation study of pure rigid polyurethane in oxidative and non-oxidative atmospheres. Journal of Analytical and Applied Pyrolysis. 2016. 120. P. 269 – 283. DOI: 10.1016/j.jaap.2016.05.015
33. Rychlý J., Lattuati-Derieux A., Lavédrine B., Matisová-Rychlá L., Malíková M., Csomorová K., Janigová I. Assessing the progress of degradation in polyurethanes by chemiluminescence and thermal analysis. II. Flexible polyether- and polyester-type polyurethane foams. Polymer Degradation and Stability. 2011. 96 (4). P. 462 – 469. DOI: 10.1016/j.polymdegradstab.2011.01.012
34. Szycher M. Szycher's handbook of polyurethanes. 2nd ed. Boca Raton, FL: CRC Press. Taylor & Francis. 2013. 17. P. 1126.
35. Chattopadhyay D. K., Webster D. C. Thermal stability and flame retardancy of polyurethanes. Progress in Polymer Science. 2009. 34 (10). P. 1068 – 1133. DOI: 10.1016/j.progpolymsci.2009.06.002
36. Fabris H.J. Thermal and oxidative stability of urethanes. Advances in Urethane Science and Technology. ed. by K.C. Frisch, S.L. Reegen. Westport, Conn.: Technomic Publishing. 1976. 4. P. 89 – 111.
37. Mathur G., Kresta J.E., Frisch K.C. Stabilization of polyether-urethanes and poly(ether-urethane-urea) block copolymers. Advances in Urethane Science and Technology. ed. by K. C. Frisch S.L. Reegen. Westport: Technomic Publication. 1978. 6. P. 103 – 172.
38. Woolley W.D. Nitrogen-containing products from the thermal decomposition of flexible polyurethane foams. British Polymer Journal. 1972. 4 (1). P. 27 – 43.
39. Ravey M., Pearce E. M. Flexible polyurethane foam. I. Thermal decomposition of a polyether-based, water-blown commercial type of flexible polyurethane foam. Journal of Applied Polymer Science. 1997. 63 (1). P. 47 – 74. DOI: 10.1002/(SICI)1097-4628(19970103)63:1<47:AID-APP7>3.0.CO;2-S
40. Awad W.H., Wilkie C.A. Investigation of the thermal degradation of polyurea: The effect of ammonium polyphosphate and expandable graphite. Polymer. 2010. 51 (11). P. 2277 – 2285. DOI: 10.1016/j.polymer.2010.03.033
41. Zhang X., Qu X., Guan Q., Li R., Wang Z., Xie H. Rigid polyurethane foam with improved thermal stability and flame retardancy modified by barium phytate and zinc oxide. Case Studies in Thermal Engineering. 2025. 72. P. 106261. DOI: 10.1016/j.csite.2025.106261

42. Jiao L., Xiao H., Wang Q., Sun J. Thermal degradation characteristics of rigid polyurethane foam and the volatile products analysis with TG-FTIR-MS. Polymer Degradation and Stability. 2013. 98 (12). P. 2687 – 2696. DOI: 10.1016/j.polymdegradstab.2013.09.032
43. Gaboriaud F., Vantelon J. P. Mechanism of thermal degradation of polyurethane based on MDI and propoxylated trimethylol propane. Journal of Polymer Science: Polymer Chemistry Edition. 1982. 20 (8). P. 2063 – 2071.
44. Moroi G., Ciobanu C. Aspects of polyesterurethane interaction with metallic ions: II. Synthesis and thermal behavior of polyurethane interaction products with manganese and copper ions. Thermochimica Acta. 2002. 385 (1-2). P. 153 – 162.
45. Moroi G. Influence of ion species on the thermal degradation of polyurethane interaction products with transition metal ions. Journal of Analytical and Applied Pyrolysis. 2004. 71 (2). P. 485 – 500.
46. Kayed S.F., Almeataq M.S. Photocatalytic Activity and Thermal Stability of Hybrid Metal-Polymer-Coordinated Complexes Derived from Gallic Acid and Ethylenediamine. Langmuir. 2023. 39 (30). P. 10445 – 10452. DOI: 10.1021/acs.langmuir.3c00869
47. Wang L.-F. Coordination and morphology of metal/polyetherurethane complexes. European Polymer Journal. 2010. 46 (12). P. 2372 – 2380. DOI: 10.1016/j.eurpolymj.2010.09.013
48. Wang Y., Song H., Ge H., Wang J., Wang Y., Jia S., Deng T., Hou X. Controllable degradation of polyurethane elastomer via selective cleavage of C–O and C–N bonds. Journal of Cleaner Production. 2018. 176. P. 873 – 879. DOI: 10.1016/j.jclepro.2017.12.046
49. Abtahi S., Hendeniya N., Mahmud S. T., Mogbojuri G., Iheme C. L., Chang B. Metal-Coordinated Polymer–Inorganic Hybrids: Synthesis, Properties, and Application. Polymers. 2025. 17 (2). P. 136. DOI: 10.3390/polym17020136
50. Pobłocki K., Pawlak M., Drzeżdżon J., Jacewicz D. Catalytic materials based on metals (ions) used in the upcycling of plastics and polymers into fuels and valuable chemicals as part of sustainable development. Materials Science and Engineering: R: Reports. 2025. 162. P. 100881. DOI: 10.1016/j.mser.2024.100881
51. Kovalchuk A.R., Ivashchuk O.S., Suprun W.Ya., Burets O.R., Reutskyy V.V. Depolymerization of rigid polyurethane waste via catalytic glycolysis in the presence of K, Na, and Ca compounds. Journal of Chemistry and Technologies. 2026. 34 (1). P. 326-332.
52. Didenko A.L., Sukhanova T.E., Nesterova A.S., Vaganov G.V., Lavrentiev V.K., Kabykhno I.A., Grozova N.A., Popova E.N., Kamalov A.M., Polotnyanshchikov K.S., Anokhina T.S., Borisov I.L., Kudryavtsev V.V. Structure-Properties Correlations in Novel Copoly(urethane-imide) Films Selectively Destructed Under Thermolysis and Hydrolysis in Alkaline Media. Polymers. 2025. 7 (3). P. 329. DOI: 10.3390/polym17030329
53. Luo W., Chen M.-J., Wang T., Yang F., Yan L., Wang Y.-Z. Catalytic polymer self-cleavage for CO_2 generation before combustion empowers materials with fire safety. Nature Communications. 2024. 15 (1). P. 2726. DOI: 10.1038/s41467-024-46756-0
54. Lu S.-Y., Hamerton I. Recent developments in the chemistry of halogen-free flame retardant polymers. Progress in Polymer Science. 2002. 27 (8). P. 1661 – 1712. DOI: 10.1016/S0079-6700(02)00018-7
55. Mustafayeva F., Kakhramanov N., Allahverdiyeva Kh., Babayeva T., Ashurova N. Fire-resistant polymer composites based on mineral fillers. RSC Advances. 2026. 16 (7). P. 6257 – 6287. DOI: 10.1039/d5ra09525e

INFORMATION ABOUT THE AUTHORS

Lipka P.A., e-mail: petr.lipka2020@gmail.com, ORCID ID: 0009-0004-3542-6762, National Research Moscow State University of Civil Engineering, Department of Construction Materials Science, PhD Student

Bruyako M.G., email: mbruyako@yandex.ru, ORCID ID: https://orcid.org/0000-0003-1284-6209, National Research Moscow State University of Civil Engineering, Department of Construction Materials Science, Candidate of Engineering Sciences (Ph.D.)

Kozlova I.V., e-mail: iv.kozlova@mail.ru, ORCID ID: https://orcid.org/0000-0001-8269-5624, SCOPUS: https://www.scopus.com/authid/detail.uri?authorId=56574815000, National Research Moscow State University of Civil Engineering, Department of Construction Materials Science, Candidate of Engineering Sciences (Ph.D.), Associate Professor

Samchenko S.V., e-mail: samchenko@list.ru, ORCID ID: https://orcid.org/0000-0002-3523-593X, SCOPUS: https://www.scopus.com/authid/detail.uri?authorId=56575166100, National Research Moscow State University of Civil Engineering, Department of Construction Materials Science, Doctor of Engineering Sciences (Advanced Doctor), Professor

Korshunov A.V., e-mail: KorshunovAV@mgsu.ru, ORCID ID: https://orcid.org/0000-0002-7585-0953, SCOPUS: https://www.scopus.com/authid/detail.uri?authorId=10042543600, National Research Moscow State University of Civil Engineering, Department of Construction Materials Science, Doctor in Chemistry (Advanced Doctor), Professor

Taran G.S., e-mail: glafi33@mail.ru, ORCID ID: https://orcid.org/0009-0007-6784-0572, SCOPUS https://www.scopus.com/authid/detail.uri?authorId=57217482062, Kurnakov institute of General and Inorganic Chemistry, Russian Academy of Sciences